UDC 621.314.1 doi:10.20998/2413-4295.2025.01.03

INCREASING THE EFFICIENCY OF A 5 KW HOME AUTONOMOUS SOLAR POWER PLANT WITHOUT A SEPARATE CHARGING CONVERTER

V. IVAKHNO[1*], V. ZAMARUIEV[1], O. PLAKHTII[2], D. VINNIKOV[3], M. DOLUDA[4], M. FILIPIEVA[2]

[1] Department "Industrial and Biomedical Electronics", NTU "KhPI", Kharkiv, UKRAINE
[2] Department "Electrical power engineering, electrical engineering and electromechanics", UkrSURT, Kharkiv, UKRAINE
[3] Department of Electrical Power Engineering and Mechatronics Tallinn University of Technology TALTECH, Tallinn, ESTONIA
[4] Viatek company, Kyiv, UKRAINE
**e-mail: Volodymyr.Ivakhno@khpi.edu.ua*

ABSTRACT *The assessment of the parameters of the power section of the converter as part of an autonomous PV plant installation with a rated power of 5000 W, designed to supply consumers with single-phase sinusoidal voltage of 220 V 50 Hz using a transformerless circuit is provided. The structure of the proposed PV plant differs from traditional structures. In the proposed structure, the DC voltage converter is connected with its input to the series connection of solar panels and performs the function of maximizing the output power and its output is connected to the DC link – the battery. The voltage-source inverter with sin pulse-width modulation is also connected to this link, its output voltage is the supply voltage of consumers. The minimum battery voltage is slightly higher than the output voltage amplitude of the DC/AC inverter. In this structure, unlike common systems with a 48V battery, there is no need for a separate bidirectional DC/DC converter with the functions of ensuring the coordination of the battery voltages and the internal DC voltage link (about 400 V, from which the voltage-source inverter is powered) and ensuring the charge – discharge of the battery with a set power from half the nominal power and above. The absence of a separate DC/DC converter simplifies the system and allows to significantly increase its efficiency in the battery load power supply mode. In the article evaluates the parameters of the PV plant of the proposed structure: the required number of serial solar panels with a nominal power of 500 W is determined, the use of a step-down DC-DC converter circuit is justified, its PWM frequency (25 kHz) is selected and the capacitance of the input storage capacitor is estimated. For the switches of the DC-DC converter, it is proposed to use modern field-effect transistors with an insulated gate and Schottky diodes based on silicon carbide (SiC); the types of semiconductor devices are selected and the power loss estimate in them (about 12 W) is provided. The required number of series-connected accumulator battery cells is determined. For the DC/AC inverter using the bridge circuit, the MOSFET type and the PWM frequency of 25 kHz are selected. The use of a three-level (unipolar) PWM algorithm is proposed, which allows doubling the output current ripple frequency. Estimates of power losses in the DC/AC inverter switches are provided: about 50 W. It is proposed to use a sendust ring core for the output filter choke, the choke parameters are determined, including an estimate of power losses: about 7 W. An estimate of the efficiency of an autonomous PV plant is provided: in the solar panel power mode 98.3% versus 97.6% for the analog and 98.8% when powered by an accumulator battery versus 94% for the analog, which corresponds to a reduction in power losses of 1.4 – 5 times.*

Keywords: *autonomous PV plant; solar panels; DC/DC converter; accumulator batteries; DC/AC voltage inverter; sin PWM; insulated gate field effect transistors; silicon carbide; power loss; sendust.*

ПІДВИЩЕННЯ ЕФЕКТИВНОСТІ ПОБУТОВОЇ АВТОНОМНОЇ СОНЯЧНОЇ ЕЛЕКТРОСТАНЦІЇ ПОТУЖНІСТЮ 5 КВТ БЕЗ ОКРЕМОГО ЗАРЯДНОГО КОНВЕРТОРА

В. В. ІВАХНО[1], В. В. ЗАМАРУЄВ[1], О. А. ПЛАХТІЙ[2], Д. ВИННИКОВ[3], М. В. ДОЛУДА[4], М. В. ФІЛІП'ЄВА[2]

[1]кафедра «Промислова і біомедична електроніка», НТУ «ХПІ», Харків, УКРАЇНА
[2]кафедра «Електроенергетика, електротехніка та електромеханіка», УКРДУЗТ, Харків, УКРАЇНА
[3]кафедра «Електроенергетика та мехатроніка» Талліннський технологічний університет, ТАЛТЕХ, Таллінн, ЕСТОНІЯ
[4] компанія «Віатек», Київ, УКРАЇНА

АНОТАЦІЯ *Дається оцінка параметрів силової частини перетворювача у складі автономної сонячної фотоелектричної установки з номінальною потужністю 5000 Вт, призначеної для живлення споживачів однофазною синусоїдальною напругою 220 В 50 Гц за без-трансформаторною схемою. Структура фотоелектричної установки, що пропонується, відрізняється від традиційних структур тим, що, що перетворювач постійної напруги, який своїм входом під'єднаний до послідовного з'єднання сонячних панелей і здійснює функцію максимізації вихідної потужності, своїм виходом під'єднаний до ланки постійного струму – акумуляторної батареї. До цієї ж ланки під'єднано автономний інвертор напруги з широтно-імпульсною модуляцією за синусоїдальним законом, його вихідна напруга є напругою живлення споживачів. Мінімальна напруга акумулятора дещо вища за амплітуду вихідної напруги інвертора напруги. У такій структурі, на відміну від розповсюджених систем з акумуляторною батареєю напругою 48В, нема необхідності у окремому двоспрямованому перетворювачі постійної напруги з функціями забезпечення узгодження напруг акумулятора і*

ISSN 2079-5459 (print)
ISSN 2413-4295 (online)

внутрішньої ланки постійної напруги (біля 400 В, від якої живиться автономний інвертор напруги) і забезпечення заряду – розряду акумулятора з встановленою потужністю від половини номінальної потужності та вище. Відсутність окремого перетворювача постійної напруги спрощує систему і дозволяє помітно підвищити ККД в режимі живлення навантаження від акумулятора. Проведені оцінки параметрів сонячної фотоелектричної установки запропонованої структури: визначено необхідну кількість послідовних сонячних панелей номінальною потужністю 500 Вт, обґрунтовано використання схеми перетворювача постійної напруги понижуючого типу, обрана його частота ШІМ (25 кГц), дана оцінка величини ємності вхідного накопичувального конденсатора. Для ключів перетворювача постійного струму запропоновано використання сучасних польових транзисторів з ізольованим затвором та діодів Шотткі на базі карбіду кремнію (SiC); вибрані типи напівпровідникових приладів та надана оцінка потужності втрат у них: приблизно 12 Вт. Визначена необхідна кількість послідовно з'єднаних комірок акумуляторної батареї. Для інвертора напруги за мостовою схемою обрано тип MOSFET, частоту ШІМ 25 кГц. Запропоновано використання алгоритму трирівневої (одно полярної) ШІМ, який дозволяє подвоїти частоту пульсації вихідного струму. Надані оцінки потужності втрат у ключах інвертора напруги: орієнтовно 50 Вт. Запропоновано для дроселя вихідного фільтра використання сендастового кільцевого осердя, визначені параметри дроселя, в тому числі оцінка потужності втрат: біля 7 Вт. Надана оцінка ККД автономної сонячної фотоелектричної установки: у режимі живлення від сонячних панелей 98,3% проти 97,6% у аналога та 98,8% при живленні від АБ проти 94% у аналога, що відповідає зменшенню втрат потужності у 1.4 – 5 разів.
Ключові слова: *автономні сонячні фотоелектричні установки; сонячні панелі; перетворювач постійної напруги; акумуляторні батареї; автономний інвертор напруги; синусоїдальна широтно-імпульсна модуляція; польові транзистори з ізольованим затвором; карбід кремнію; потужність втрат; сендаст*

Introduction

The general direction of world energy development is related to the wide use of renewable energy sources. This is due to the growth of demand for electricity with a simultaneous increase in efforts to eliminate emissions of conventional pollutants, decarbonize electricity as a replacement for fossil fuels in transport, construction and industry. The dynamics of commissioning of solar power plants in recent years significantly exceeds this indicator for other renewable energy sources and this trend will continue. It is expected that in the European Union the growth of rooftop solar photovoltaic installations will outpace the growth of large-scale power plants [1]. For Ukraine, the use of an autonomous solar photovoltaic installation is particularly relevant due to damage to the power infrastructure, interruptions in power supply, etc. as a result of the aggression of the Russian Federation.

Typically, all solar PV plants are divided into residential, with a capacity of 3-11 kW, commercial – 100 kW-2 MW and municipal scale – 5-100 MW [2]. Plants used in the residential sector, as a rule, have a battery as an intermediate energy storage - a local battery energy storage system, which allows to powered the domestic electricity consumers in the absence of grid energy. Commercial and municipal solar PV plants can use external battery energy storage systems to smooth out peaks in electrical energy consumption.

The difference in the functionality of solar PV plants is due to their different structures and circuit solutions of semiconductor energy converters used in the plants. The most universal solar PV plant is a hybrid solar PV plant. Unlike hybrid structures, the autonomous PV plant, also called solar PV plants, have a similar structure, but are not designed to transfer excess energy generated in the solar PV plant to a single-phase alternating current network with a frequency of 50 Hz. Their inverter is not designed for connection to the AC grid, and its load is household appliances. In the European Union and some countries of the world, residential solar PV plants of this structure are limited to a capacity of 10 kW [3]. This paper considers autonomous solar PV plant structures with a capacity of about 5 kW, as one of the most widely used for alternative power supply of private households, for example, in rural areas.

A typical structure of a solar PV plant is shown in Fig. 1 [4]. Autonomous solar PV plants, as a rule, have the structure of a two-stage converter with input stage constant voltage converters (DC/DC) as input stage, the number of which corresponds to the number of connected strings of serially connected solar panels (PV strings) and which also perform the function of finding the point with maximum power (Maximum Power Point Tracker, MPPT). DC/DC converters operate to a DC link (DC-coupled system). To DC link a DC/AC converter is connected with or without a built-in matching transformer. Depending on the availability of grid energy, the domestic electricity consumers is powered either from the grid or from the solar PV plant. Switching is performed using switching devices, which are not shown in the Fig. 1.

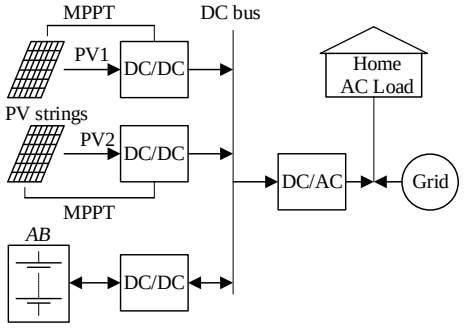

Fig. 1 – Typical structure of a solar PV plant [4]

The battery pack or battery energy storage system is connected to the DC link using a separate DC/DC converter, which has the functions of regulating the charge-discharge current of the battery, ensuring the coordination of the voltage of the battery and the internal

DC bus, and transferring energy from the battery energy storage system to the DC link in the event of insufficient energy from the solar panels and/or lack of grid energy.

The solar PV plant BluE H3/H5 manufactured by KSTAR [5] has a similar structure. These systems use batteries with a nominal voltage of 48 V and a voltage range of 40 to 60 V. This voltage is a compromise between the overall cost of operating the batteries, the cost of the DC/DC converter, and the efficiency of the system. The presence of a separate DC/DC converter complicates and increases the cost of the entire system and does not contribute to improving the efficiency. Thus, according to the specification of the solar PV plant BluE H3/H5 [5], the maximum efficiency when powering the load from the battery is 94%, and from photo panels – 97.6%, that is, the latter is significantly higher.

There are several typical structural schemes of a solar PV plant [4,6,7]. This paper considers the structure of a solar PV plant with a DC link, without a separate DC/DC converter serving the battery (Fig. 2).

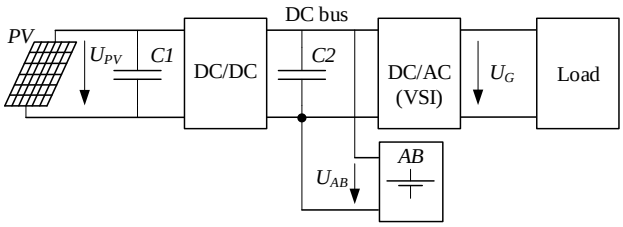

Fig. 2 – Simplified diagram of the solar PV plant under consideration

Solar PV plant includes a PV photo panel block, a DC voltage converter block (single-link DC/DC converter with MPRT function), a battery block, an autonomous DC/AC inverter (Voltage Source Inverter, VSI) with sinusoidal PWM. Power of the solar PV plant is 5000 W, output voltage – 220 V, 50 Hz.

Work Purpose

The purpose of the work is to evaluate the main parameters of the solar PV plant under consideration, including power losses and efficiency. Proposals are formed for the selection of types of power semiconductor switches and parameters of passive elements.

Evaluation of battery parameters, solar panels and selection of DC-DC converters

The voltage of the DC link in converters with the structure of Fig. 1 is determined, usually, only requirements from the DC/AC converter. In converters with the structure of Fig. 2, these requirements are significantly influenced by the characteristics of the batteries. In our case, the range of battery voltage changes should be such that this voltage U_{AB} is not less than the minimum amplitude of the output voltage U_{Gm}^{min}=220·1,41·0,9=280 V. It is advisable to give a reserve of 10%, then the minimum battery voltage should be U_{AB}^{min} = 310 V.

Let us assume that the battery cells are made using $LiFePO_4$ technology. The minimum voltage of one element is U_{cell}^{min} = 3.0 V (10% of residual capacity), the nominal voltage – U_{cell}^{nom} =(3.20 ~ 3.25 V), and the maximum – is U_{cell}^{max} =3.65 V (Fig. 3).

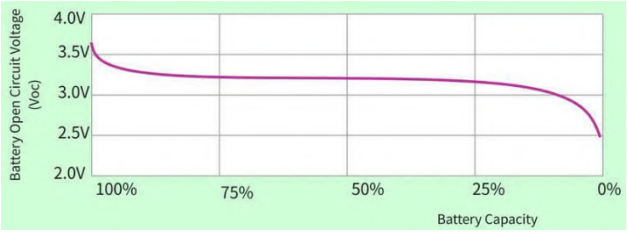

Fig. 3 – Dependence of the voltage of a 3.2V $LiFePO_4$ cell on the degree of discharge of the battery [8]

We set the minimum cell voltage at 3.0 V. Then the number of series-connected elements $N_{AB}=U_{AB}^{min}/U_{cell}^{min}$ =310/3=103. Alternatively, we can assume a series connection of 26 sections with 4 cells per section (N_{AB}=26·4=104; $U_{AB}^{min}= N_{AB}\cdot U_{cell}^{min}$=104·3=312 V), batteries with a series connection of 4 cells with a nominal section voltage of 12.8 V and a total nominal voltage U_{AB}^{nom}=3,2·104=333 V may be available. Taking this into account, we can assume the following values of the minimum and maximum battery voltage: U_{AB}^{min} =312 V, U_{AB}^{max}=3,65·104=380 V. Assuming that the installed capacity of the battery is the same as in system [5], i.e. its base nominal voltage is 50 V, and the base capacity is 100 A∗h and the energy is E=5000 W∗h, at a voltage of U_{AB}^{nom} =333 V we find an estimate for the capacity of the battery: $C_{AB}=E/U_{AB}^{nom}$ =5000/333=15 A∗h: the battery should consist of 104 series-connected cells with a capacity no less than 15 A∗h.

It should be noted that the features of $LiFePO_4$ batteries are the high repeatability of cell parameters, which makes it possible to exclude the use of active BMS (Battery Management System) balancers for capacities less than 40 A∗h. It is possible to manufacture such a "non-standard" battery of 104 cells at the facilities of Viatec [9], which specializes, in particular, in the distribution and manufacture of components for solar energy.

Of the two main types of DC-DC converters (DC/DC converter unit with MPRT function, see Fig. 2) – boost or buck – in the opinion of the authors, it is advisable to choose a buck-type DC-DC converter, since such a DC-DC converter has an output choke that is connected to the positive output of the battery. The choke limits the current ripple when charging the battery, which has a beneficial effect on the battery. In addition, limiting the ripple of the output current of the DC-DC converter helps reduce the share of inactive components of the

ISSN 2079-5459 (print)
ISSN 2413-4295 (online)

system power, which, in turn, helps increase the efficiency of the system [10].

For the structure of Fig. 2 with a step-down *DC-DC* converter, the minimum voltage of the solar panel strings U_{PV}^{min} must be no less than the maximum battery voltage: $U_{PV}^{min} > U_{AB}^{max}$=380 V.

It is known that the main parameters of solar panels, which are displayed in the specifications, are divided into two groups: found for the STC mode (Standard Test Conditions: solar intensity 1000 W/m^2, photovoltaic cell temperature 25°C) or NOCT (Normal Operating Cell Temperature), which is determined under the conditions: solar intensity 800 W/m^2, ambient temperature 20°C. The temperature of the photovoltaic cell depends on its characteristics and is higher than the air temperature by 10–30°C) [11]. The specific temperature is given in the documents for solar panels.

Let us choose as the base panel PNGNH60-B8(182) from Hefel Pinergy Solar Technology Co., Ltd, China with a nominal power (in STC mode) of 500 W [12]. According to the specification, the NOCT power is 376 W, the temperature coefficient of voltage for the maximum power point TK_U is TK_U=-0,28%/°C, the NOCT temperature $T_{(NOCT)}$=44°C, the voltage at maximum power of the MPPT in STC mode $U_{MP}^{(25℃)}$ =36.06 V, the voltage at maximum power of the MPPT in NOCT mode $U_{MP}^{(44℃}$ =33.91 V, the maximum temperature is 70°C. Then the estimate for the voltage for maximum power at 70°C is:

$$U_{MP}^{(T℃)} = U_{MP}^{(44℃)} + TK_U(T - T_{(NOCT)}),$$
$$U_{MP}^{(70℃)} = 33{,}91 - 0{,}0028(70 - 44) = 33{,}84\text{V} \qquad (1)$$

which differs from the voltage $U_{MP}^{(44℃)}$ =33.91 V by only 0.1 V, i.e. insignificantly. It can be stated that for modern PVs the effect of temperature on the voltage in the maximum power mode at the temperature for the NOCT mode and higher temperatures is insignificant.

Let us assume the minimum voltage of one panel $U_{PV(1)}^{min}$ at the level of 32 V (with some margin): $U_{PV(1)}^{min}$ =32 V.

To ensure the requirement $U_{PV}^{min} > U_{AB}^{max}$ =380 V, it is necessary to install N panels in series: $N = U_{PV}^{min}/U_{PV(1)}^{min}$ =380/32=11.88, i.e. N=12, while the voltage of the series connection of 12 PVs (PV string) will be 12·32=384 V. The nominal installed power P_{PV}^{nom} (STC mode) will be $P_{PV}^{nom} = P_{PV(1)}^{nom} \cdot N$=500·12=6000 W, and for the NOCT mode for one panel (radiation 800 W/m2, voltage $U_{MP(1)}^{(44℃)}$=33.91 V, current $I_{MP}^{(44℃)}$=11.09 A, power $P_{MP(1)}^{(44℃)}$=376 W) the operating power $P_{PV}^{NOCT} = P_{MP(1)}^{(44℃)} \cdot N$=376·12=4512 W.

Requirements for the class of DC/DC switches and assessment of their main parameters

The simplified diagram of the input block of a solar photovoltaic installation is shown in Fig. 3. It includes solar panels, a DC/DC converter with MPPT function and a battery. When used as a DC/DC converter – a buck converter of constant voltage, the maximum voltage that can be applied to the keys *VT1, VD1* is equal to the voltage of the PV string of 12 panels.

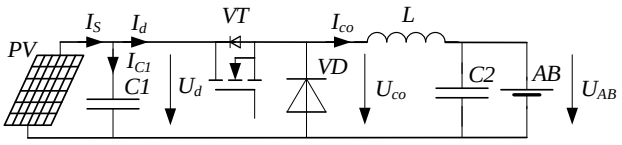

Fig. 3 – Simplified diagram of the input block of a solar PV plant

In the no-load mode of the STC mode, the no-load voltage $U_{PV(1)}^{xx}$ of one PV, according to the specification, is $U_{PV(1)}^{xx}$ =43.39 V, and for a string with N=12 PVs – $U_{PV}^{xx} = U_{PV(1)}^{xx} \cdot N$=43,39·12=520 V.

Fig. 4 shows a family of volt-ampere characteristics of PVs for a power of 435 W for different temperatures [12].

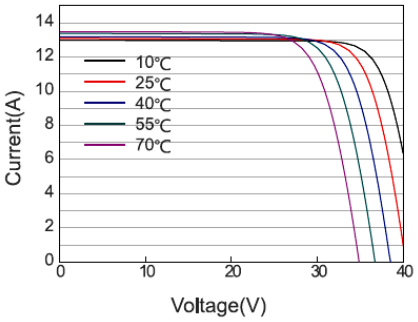

Fig. 4 – Family of current-voltage characteristics of the PV

Extrapolating the curve of the dependence of the PV current on the voltage for a temperature of 10°C (Fig. 4) for the idle mode (XX), we see the approximate value of the XX voltage in this case – 45 V. The latter gives the maximum value of the string voltage of 540 V. Thus, keys (diodes and MOSFET transistors) with a limit voltage of y 650 – 700 V can be used as keys, especially since the actual switching of the keys will occur at voltages close to $U_{MP}^{(25℃)}$ = 36.06 V and below (with increasing temperature), which gives an approximate value of the string voltage $U_{MPS}^{(25℃)}$ at which switching is performed $U_{MPS}^{(25℃)} = U_{MP}^{(25℃)} \cdot N$=36,06·12=432 V, and in the NOCT mode $U_{MPS}^{(44℃)} = U_{MP}^{(44℃)} \cdot N$=33,91·12=407 V. At PV voltages exceeding 40 V (string voltage 480 V), switching can be omitted at all, without turning on the transistor.

Let's estimate the main parameters of the switches in order to determine the its types. The class of switches is determined - about 700 V. We will find other parameters for the NOCT mode for the PV (at the string voltage $U_{MPS}^{(44℃)} = U_d$ = 407 V, the panel (string) current $I_S^{(44℃)} = I_S$ = 11.09 A. Let's set the battery voltage $U_{AB} = U_{AB}^{nom}$ = 333 V. At this stage, we consider the

switches *VT*, *VD* to be ideal, the capacitances of the capacitors *C1*, *C2*, and the inductance of the choke *L* to be large (i.e., the ripples of the input voltage of the DC-DC converter U_d and the output current of its switch I_v are insignificant).

The average value of the switch voltage U_{co} over the period *T* of the *f* PWM frequency coincides with the value of the voltage AB: $U_{co}=U_{AB}^{nom}$ = 333 V. The value of the duty cycle τ of the transistor current pulse is found from the equation for switch voltages:

$$U_в=\tau U_d\,, \quad \tau=U_в/U_d=333/407=0{,}82 \qquad (2)$$

Fig. 5 shows the time diagrams of currents and voltages in the DC-DC converter according to Fig. 3: transistor gate voltage *VT* u_{GVT} (Fig. 5a), capacitor current C1 i_{C1} (Fig. 5b), transistor current VT i_{VT} (Fig. 5c), switch output voltage u_{co} (Fig. 5d) and choke voltage L u_L (Fig. 5e).

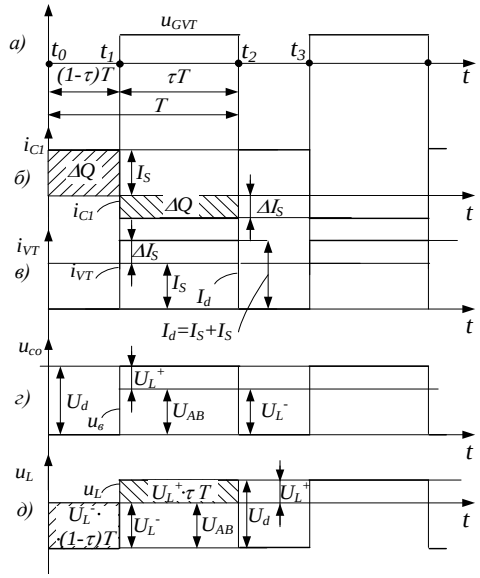

Fig. 5 – Timing diagrams of processes in a DC-DC converter

Let the transistor *VT* be turned on by the moment t_0, through it, the choke *L* and the battery a current I_d flows, the panel current has the value I_S, the voltage of the panel and capacitor *C1* is U_d. At the moment t_0 the transistor *VT* is turned off, the diode *VD* is turned on and the panel current I_S begins to flow through the capacitor *C1*. The choke current of the value I_d continues to flow through the battery, charging it, the voltage on the choke becomes equal to the battery voltage.

At the moment t_1 the transistor *VT* is turned on, the diode *VD* is turned off. During the interval t_1- t_0 with a duration of $(1-\tau)T$, an additional charge of the value $\Delta Q=(1-\tau)\cdot T\cdot I_S$ accumulates in the capacitor. This charge during the interval t_2- t_1 with a duration of τT, until the transistor is turned off at the moment t_2, is transferred to the load by the current ΔI_S. Thus, an additional component ΔI_S appears in the current I_d: $I_d = I_S+\Delta I_S$. An estimate for the value ΔI_S can be made on the basis of the balance (equality) of charges of value ΔQ, which enter the capacitor *C1* in the interval t_2- t_1 with a duration of $(1-\tau)T$ and are removed from it in the interval t_1-t_0 with a duration of τT:

$$\Delta Q=(1-\tau)\cdot T\cdot I_S=\tau T\cdot\Delta I_S, \qquad \Delta I_S=((1-\tau)/\tau)\cdot I_S \qquad (3)$$

For I_S=11,09 A, τ=0,82

$$\Delta I_S=((1-\tau)/\tau)\cdot I_S=((1-0{,}82)/0{,}82)\cdot 11{,}09=2{,}43\ \text{A},$$
$$I_d=I_S+\Delta I_S=11{,}09+2{,}43=13{,}52\ \text{A}.$$

Average I_{AVVT}, effective I_{RMSVT} current of the transistor and average I_{AVVD}, effective I_{RMSVD} current of the diode:

$$I_{AVVT}=(I_S+\Delta I_S)\cdot\tau=(11{,}09+2{,}43)\cdot 0{,}82=11{,}09\ A\,,$$
$$I_{RMSVT}=(I_S+\Delta I_S)\cdot\sqrt{\tau}=(11{,}09+2{,}43)\cdot\sqrt{0{,}82}=12{,}2\ A$$
$$I_{AVVD}=(I_S+\Delta I_S)\cdot(1-\tau)=(11{,}09+2{,}43)\cdot(1-0{,}82)=2{,}43\ A$$
$$I_{RMSVD}=(I_S+\Delta I_S)\cdot\sqrt{1-\tau}=(11{,}09+2{,}43)\cdot\sqrt{1-0{,}82}=5{,}31\ A$$

Selecting the type of DC/DC diode (MPPT)

When using a PWM frequency above 20 kHz, the frequency properties of the diode play an important role, in particular, the value of the reverse recovery charge $Q_{rr.}$, the value of which is responsible for the losses in the transistor when it is forced to turn on, which results in the diode turning off. At a finite value of this charge, the effect of through currents occurs, and the power of the transistor's turn-on losses can often, at high frequencies, constitute a significant portion of all converter losses. Devices that fundamentally do not have this charge are attractive – Schottky diodes. Currently, Schottky diodes based on silicon carbide (SiC) technology are available on the market, which, like silicon ones, do not have a charge $Q_{rr.}$, but have an increased reverse voltage U_{RR} from 650 – 1200 V and higher, have an acceptable price – 0.2-0.6 $/A of the classification current (for a voltage of 650 V), a voltage drop U_F of about 1.5 V.

Let's choose as the *VD* diode a diode of the IDH12G65C6 type from *Infineon* [13] with the main parameters: U_{RR} = 650 V, a voltage drop U_F of about 1.5 V, capacitance energy at a voltage of 400 V E_C = 3.2 μJ, cost $ (1.9 – 5.05) [14]. Let's assume the operating junction temperature T_j=100 °C. According to the graphs of the I-V family at T_j=100 °C and I_F= I_d =13.52 A, the voltage drop U_F will be U_F =1.4 V. The average power of static losses $P_{VD(st)}$

$$P_{VD(st)}=U_F\cdot I_d\cdot(1-\tau)=1{,}4\cdot 13{,}52\cdot(1-0{,}82)=3{,}4\ \text{Вт} \qquad (4)$$

Let us take the approximate value of the PWM frequency *f* = 25000 Hz. At the operating reverse voltage of the diode U_R= U_d =407 V, according to the specification, the energy E_C accumulated in the diode capacitance is about 3.2 μJ: $E_C=3{,}2\cdot 10^{-6}$ J. At the frequency *f* = 25000 Hz, this energy is released in the diode in the form of heat in each period. Average additional power $P_{VD(C)}$:

ISSN 2079-5459 (print)
ISSN 2413-4295 (online)

$$P_{VD(C)} = E_C \cdot f = 3{,}2 \cdot 10^{-6} \cdot 25000 = 0{,}08 \text{ W} \quad (5)$$

and is not significant. Power loss in the diode will be:

$$P_{VD} = P_{VD(st)} + P_{VD(C)} = 3{,}4 + 0{,}08 = 3{,}48 \text{ V} \quad (6)$$

Selecting the type of DC/DC transistor (MPPT)

SiC-based MOSFETs are currently available on the market, which have the following advantages: ultra-low switching losses; low gate threshold voltage, $V_{GS(th)}$ = 4.5 V; resistance to parasitic turn-on even at a gate turn-off voltage of 0 V; high operating junction temperature T_j (up to 175 °C). Transistors with a cut-off voltage of 650 – 1200 V are available. As the *VT* transistor, we will choose a transistor of the IMZA65R040M2H type from Infineon [15] with a price of about $(4.6–9.7) [16] with the following main parameters: cut-off voltage V_{DSS} = 650 V, nominal channel resistance $R_{DS(on)}$ =40 mΩ, energy when switching off $E_{VT(off)}$ at a leakage current $I_{DS}=I_d$ =13.52 A and a voltage of 400 V (which is close to the switching voltage U_d = 407 V) $E_{VT(off)}$ =11 μJ. Assuming the operating temperature of the crystal T_j=100 °C, after correcting the channel resistance to this temperature, we obtain the operating resistance value: $R_{DS(on)}^{(100°C)}$= 52.5 mΩ and an estimate for the voltage drop of the switched-on device: $U_{VT(on)}=I_d \cdot R_{DS(on)}^{(100°C)}$=13,52·0,0525=0,71 V. Estimate for the static power loss $P_{VT(st)}$

$$P_{VT(st)} = I_{RMSVT}^2 \cdot R_{DS(on)}^{(100°C)} = 12{,}2^2 \cdot 0{,}0525 = 7{,}8 \text{ W} \quad (7)$$

Estimated power loss of switching off at a voltage U_{DS}=400 V (which is practically no different from the voltage U_d =407 V, the specification indicates the energy value $E_{VT(off)}$ =11 μJ):

$$P_{VT(off)} = E_{VT(off)} \cdot f = = 11 \cdot 10^{-6} \cdot 25000 = 0{,}275 \text{ W} \quad (9)$$

In the specification, the turn-on losses are given for the transistor in the DC-DC converter, taking into account the effect of the reverse recovery charge of the MOSFET diode. In this case, the diode is used without this charge, so we assume that the turn-on losses $E_{VT(on)}$ coincide with the turn-off losses: $E_{VT(on)}=E_{VT(off)}$. Then the switching power losses $P_{VT(sw)}$ will be:

$$P_{VT(sw)} = 2\, P_{VT(off)} = 2 \cdot 0{,}275 = 0{,}55 \text{ W} \quad (10)$$

Let us also take into account the losses associated with the discharge of the output capacitance C_{oss} of the transistor. According to the specification, the energy P_{Coos} for a voltage of 400 V is 7 μJ. Then the power value P_{Coos} will be

$$P_{Coos} = P_{Coos} \cdot f = 7 \cdot 10^{-6} \cdot 25000 = 0{,}175 \text{ W} \quad (11)$$

Total power loss P_{VT}:

$$P_{VT} = P_{VT(st)} + P_{VT(sw)} + P_{Coos} = 7{,}8 + 0{,}55 + 0{,}175 = 8{,}53 \text{ W} \quad (12)$$

Capacitance estimation of the capacitor *C1* and the inductance of the choke *L*

Simplified diagrams of capacitor voltage and inductor current over the PWM frequency period are presented in Fig. 6a and 6b, respectively.

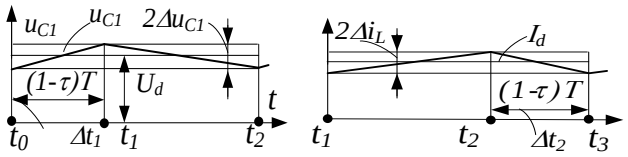

а) *б)*

Fig. 6 – Timing diagrams of processes in a DC-DC converter

We set the value of the capacitor voltage ripple coefficient $k_{пн}=\Delta u_{C1}/U_d$ at the level of $k_{пн}$=0,01. Considering that during the time interval $t_1 - t_0=\Delta t_1=(1-\tau)T$, during which the capacitor is charged by the current I_S of the PV panel, the increase in its voltage is $2\Delta u_{C1}$, we find the required capacitance value:

$$C_1 = I_S \cdot (1-\tau)/(2 \cdot k_{пн} \cdot U_d \cdot f) = = 11{,}09 \cdot (1-0{,}82)/(2 \cdot 0{,}01 \cdot 407 \cdot 25 \cdot 10^3) = 9{,}08 \cdot 10^{-6} \text{F} \quad (13)$$

i.e. 10 μF.

By analogy, with the same value of the ripple coefficient of the choke current $k_{ni}=\Delta i/I_d$ =0.01, we find the required value of inductance:

$$L = U_{AB} \cdot (1-\tau)/(2 \cdot k_{ni} \cdot I_d \cdot f) = = 333 \cdot (1-0{,}82)/(2 \cdot 0{,}01 \cdot 13{,}52 \cdot 25000) = 8{,}87 \cdot 10^{-3} \text{ H} \quad (14)$$

For the choke, since the selected value of k_{ni} is sufficiently small, the amplitude of the variable component of induction in the choke core will also be small, which will allow us to neglect hysteresis and eddy current losses in the core and eddy current losses in the winding, taking into account only ohmic losses. Since the ratio of the powers of dynamic and static losses in the transistor and diode at a given PWM frequency turned out to be quite small, there are grounds for increasing this frequency, which will allow us to reduce the installed power and mass of the reactive components of the DC-DC converter. Optimization of the DC-DC converter parameters is not part of the purpose of this work.

Selection of the circuit and the basic algorithm of the voltage-source inverter

The traditional bridge circuit of a voltage-source inverter with MOSFET power switches is shown in Fig. 7.

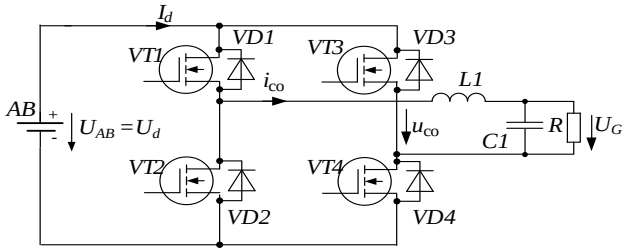

Fig. 7 – Power section diagram of a voltage-source inverter

As the basic algorithm for controlling the *VT1-VT4* switches, we will take the algorithm of unipolar (according to the terminology [7]), or three-level (according to the terminology [17]) sinusoidal pulse width modulation (SPWM). This method of signal formation uses a comparison on comparators of a carrier voltage signal of a symmetrical triangular shape with a frequency f_M with two antiphase sinusoidal voltages with amplitudes equal to the amplitude of the carrier multiplied by the modulation coefficient K_M ($K_M=U_{GM}/U_d$ where U_d is the input voltage, U_{GM} is the amplitude of the output sinusoidal voltage U_G). The output signals of the two comparators are the signals of the switching functions of the transistors for each of the two inverter racks. One of the essential features of this method of forming control signals for transistors is that the frequency of the highest harmonic of the output voltage is twice the modulation frequency (i.e., for example, twice of 25 kHz) (see Fig. 7 [18]), this allows us to significantly reduce the dimensions of the components of the power filter L_1C_1. The ratios of the average and active currents of the keys for an ideal output filter are the same as for a single-phase half-bridge inverter, the operation of which is characterized by bipolar modulation.

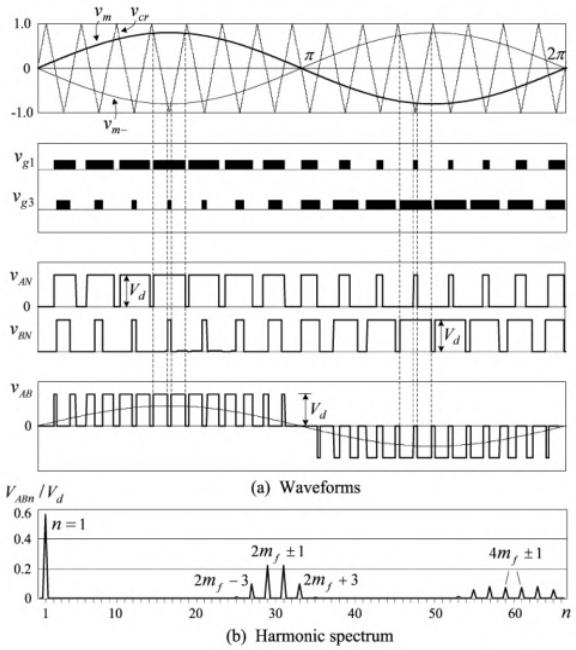

Fig. 8 – Formation of the output voltage of an voltage-source inverter for three-level PWM (carrier and bending frequency ratio 15, modulation factor 0.8 [18])

For an ideal output filter, we will assume that the output current is a sinusoid with a frequency of 50 Hz and the corresponding amplitude I_{Gm}, the load is purely active, and the output voltage is a sinusoid with an amplitude U_{Gm}. For the nominal mode

U_G =220 V, U_d= U_{AB}^{nom}=333 V, $U_{Gm} = \sqrt{2}\ U_G$ =310 V,

$$K_M = \frac{U_{Gm}}{U_d} = \frac{310}{333} = 0{,}93,\ I_{Gm} = \frac{2 \cdot P_{PV}^{NOCT}}{K_M \cdot U_d} = \frac{2 \cdot 4512}{0{,}93 \cdot 333} = 29{,}1\ A \quad (15)$$

where I_{Gm} is the amplitude of the output current; K_M is the modulation coefficient.

Key type selection and loss capacity estimation

As transistors *VT1-VT4*, we will choose MOSFET transistors using SiC technology, for which the standard voltage class is considered to be the value of the drain-source limit voltage U_{DSS} =650 V, which gives a sufficient voltage margin compared to the battery voltage amplitude U_{AB}^{max} =380 V. To gain a competitive advantage over an inverter based on IGBT of a similar voltage class (about 600 V) in terms of static key losses, we will select transistors with an average voltage drop when an average current flows $I_{вAV}=I_{вт}\cdot 2/\pi$=18,23 A of about 1 V (as opposed to the approximate value of the voltage drop on an IGBT of the class of about 600 V, about 1.7 V for low-frequency devices and about 2 V for high-frequency ones). Then the channel resistance $R_{DS(on)}$ should not be greater than:

$$R_{DS(on)} \le {}^{1}\!/_{I_{вAV}} = {}^{1}\!/_{18.23} = 0{,}054\ \Omega \quad (16)$$

Let us take as transistors *VT1-VT4* a device of type IMZA65R040M2H [15] - the same as for the MPRT converter, which for the transition temperature T_j=100 °C has $R_{DS(on)}^{(100°C)}$=52,5 mΩ.

From the specification of the IMZA65R040M2H device, it can be seen that in the current range up to 30 A, the drop across the key when current flows through the internal diode of the transistor, the voltage drop across the device (up to about 4.5 V) significantly exceeds the voltage drop when the same current flows through the gate-switched transistor (up to about 2 V). To reduce static losses, it is advisable to turn on the transistor at the gate when reverse current flows, as is done in synchronous rectifiers, and to assume that the switch current flows through the channel of the switched-on transistor both with forward and reverse switch current.

To estimate the current of the switch and the power of static losses, we will use the well-known expressions for the current of the transistor and diode in the inverter rack for bipolar PWM according to the sinusoidal law [19], assuming the threshold voltage of the on-swtch $U_{(TO)}$ = 0 and for the differential resistance of both the transistor and the diode $r_T=r_D=R_{DS(on)}^{(100°C)}$=52,5 mΩ, as well as the value of the load power factor $cos\varphi$ =1. Then:

ISSN 2079-5459 (print)
ISSN 2413-4295 (online)

$$I_{VTRMS} = I_{вт} \cdot \sqrt{\frac{1}{8} + \frac{K_M}{3 \cdot \pi}} = 29{,}1 \cdot \sqrt{\frac{1}{8} + \frac{0{,}93}{3 \cdot \pi}} = 13{,}76 \text{ A},$$

$$I_{VDRMS} = = I_{вт} \cdot \sqrt{\frac{1}{8} - \frac{K_M}{3 \cdot \pi}} = 29{,}1 \cdot \sqrt{\frac{1}{8} - \frac{0{,}93}{3 \cdot \pi}} = 4.72 \text{ A}$$

$$P_{VT\,st} = I_{VTRMS}^2 \cdot r_T = (13{,}76)^2 \cdot 0{,}053 = 10\,W$$

$$P_{VDst} = I_{VDRMS}^2 \cdot r_D = (4.72)^2 \cdot 0{,}053 = 1{,}18\,W \qquad (17)$$

Total static losses in the transistor and in the commutator:

$$P_{st}^{\ 1} = P_{VTst} + P_{VD(st)} = 10 + 1{,}18 = 11{,}2\,W$$

$$P_{st}^{\ tot} = 4 \cdot P_{st}^{\ 1} = 4 \cdot 11{,}2 = 44{,}8\,W \qquad (18)$$

The dynamic losses during transistor on/off can be estimated based on the dependence of switching energies on the value of the switched current at a switched voltage of 400 V (see Fig. 9, [15]).

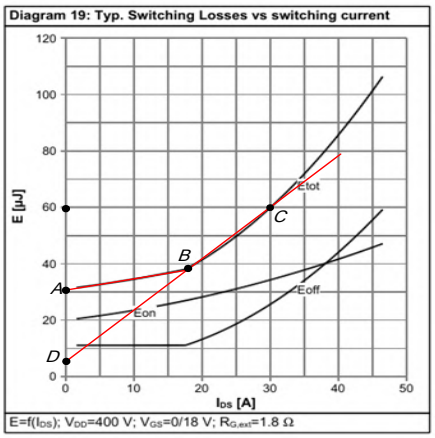

Fig. 9 – Dependence of switching loss energy on current [15]

Let us assume the PWM frequency value to be the same as for the DC-DC converter f_M = 25 kHz: The value of the total energy of switching on and off losses E_{tot}, as can be seen, linearly depends on the value of the switched current, but with two different derivatives: for the current interval from 0 to 18 A (points *A* and *B* of the graph, derivative k_1) and from 18 and 30 A (points *A* and *C* of the graph, derivative k_2). Having obtained from the graph the numerical values of the derivatives and displacement energies $E(A)=31 \cdot 10^{-6}$ J, $E(B)=39 \cdot 10^{-6}$ J, $E(D)=6 \cdot 10^{6}$ J, $k_1=0{,}39 \cdot 10^{-6}$ J/A, $k_2=1{,}75 \cdot 10^{-6}$ J/A, and also for the current of point *B* $i(B)$ =18 A, we can find the value of the angle θ_1, which corresponds to this current for the sinusoid of the current $i(\theta)=I_{вт} sin\theta$ with the amplitude $I_{вт}$ =29 A:

$$\theta_1 = \arcsin \frac{I(B)}{I_{вт}} = \arcsin \frac{18}{29} = 0.667 \text{ rad}$$

and the sum of the two energies E_1 and E_2 of the switching at angular intervals from 0 to θ_1 and from θ_1 to $\pi/2$ of the period:

$$E_1 + E_2 = = \frac{1}{2\pi} \int_0^{\theta_1} [E_A + k_1 \cdot i(\theta)] d\theta + \frac{1}{2\pi} \int_{\theta_1}^{\pi/2} [E_D + k_2 \cdot I_{вт} \sin(\theta)] d\theta$$

$$= 3.677 \cdot 10^{-6} + 7.232 \cdot 10^{-6} = 10{,}9 \cdot 10^{-6} \text{ J} \qquad (19)$$

It is known [20] that the amount of switching energy for IGBT depends on the switched voltage as a step function of the ratio of the switched and nominal voltages with the power exponent K_U =1.4. For SiC MOSFETs, such data are not available, but for Si MOSFETs, K_U =1 is assumed. Assuming K_U =1, then, taking into account the correction, we obtain an estimate of the dynamic swtch loss power:

$$P_{(tot)} = f_M \cdot 2 \cdot (E_1 + E_2) \left(\frac{U_d}{U_{DSnom}} \right)^{K_U} = 25 \cdot 10^3 \cdot 2 \cdot (3.68 \cdot 10^{-6} +$$

$$+ 7.23 \cdot 10^{-6}) \cdot \left(\frac{333}{400} \right)^1 = 0.454\,W \qquad (20)$$

Let us also take into account the power losses in the transistor, which are due to the output capacitance of the transistor. When the transistor is turned on at a voltage of U_d , the energy E_{oss}, which was accumulated in the output capacitance C_{oss}, is dissipated as heat. The device specification provides a dependence of the value of this energy on the voltage, at a voltage of U_d =333 V, the value of the energy E_{oss} will be approximately 5.3 µJ: $E_{oss}=5{,}3 \cdot 10^{-6}$ J, and the power of these losses P_{oss} is a larger value in f_M times, i.e. $P_{oss} = E_{oss} \cdot f_M = 5{,}3 \cdot 10^{6} \cdot 25 \cdot 10^{3} = 0{,}123$ W. In one transistor, the total P_{Σ}^{1} (static $P_{st}^{\ 1}$, dynamic $P_{(tot)}^{\ 1}$ and "capacitive" $P_{oss}^{\ 1}$) will be $P_{\Sigma}^{1} = P_{st}^{\ 1} + P_{oss}^{\ 1} = 11{,}8 + 0{,}123 = 12{,}4$ W, and in four transistors - 4 P_{Σ}^{1}=49,6 W - about 1% of the output power.

It should also be noted that the selected circuit of the bridge voltage-source inverter is bidirectional, i.e. it allows charging the battery from the alternating sinusoidal voltage network, which can be the source U_G (see Fig. 7). The assessment of the relevant parameters of the voltage-source inverter, which will work in this case as a regenerative rectifier, is not part of the purpose of this work.

Evaluation of the main parameters of the filter choke

We are talking about the choke L_1 of the circuit in Fig. 7, its main function is to suppress the higher harmonics of the output current. The peculiarity of the algorithm for controlling the keys of an voltage-source inverter is that the pulsating component of the current (higher harmonic currents) has a characteristic spectrum (shown in Fig. 8), in which there are higher harmonics with numbers $2m \pm 1$, where $m=f_M/f_G$, is the multiplicity of

the modulation frequency f_G relative to the envelope frequency f_G; in this case, f_G =50 Hz, f_M = 25 kHz, i.e. m=500 and $2m$=1000 and the average frequency of the higher harmonics is 50 kHz. It is to this frequency that the filter should be adjusted.

With a sufficiently large capacitance of the capacitor C_1 of the output filter (see Fig. 7), when almost all the higher harmonics of the output current of the switch flow through this capacitor, and the useful component of the sinusoidal current with a frequency of f_G is supplied to the load, the choke current as the sum of the currents of the components with a frequency of f_G and higher harmonics has a characteristic shape. Fig. 10 shows as an example the corresponding machinograms of currents that were obtained in the MATLAB package with the following parameters: R=53 Ohm, L_1=1.2 mH, C=20 μF, , f_M =5 kHz, , f_G =50 Hz [21], including the current of higher harmonics of the choke (Fig. 10 c).

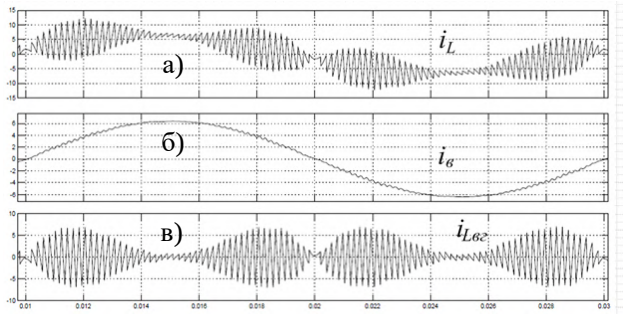

Fig. 10 – Machine diagrams of currents in the inverter at resistive load: a) - choke current; b) - output current (load current); c) - current of higher harmonics of the choke and capacitor

In relation to the output voltage of the commutator $u_в(\theta)=U_{вм}\cdot\sin\theta=K_M\cdot U_d\cdot\sin\theta$ in the range of angles (0-π) and (π-2π) the operation of the converter does not differ from the operation of the step-down converter with sinusoidal law of the change of the output voltage: the relative duration $\tau=u_в/U_d$ of the output voltage pulse as a function of the current angle θ also changes according to the sinusoidal law: $\tau(\theta)= K_M\cdot\sin\theta$. It is known [22] that during the conversion period T_P, the maximum value of the relative ripple component of the output current, i.e. k_{Pimax} depends on the value τ, according to the expression

$$k_{Pi}=\frac{\Delta i/2}{i_{co0}}=\frac{U_d(1-\tau)\tau}{2f_P L i_{co0}}, \qquad (21)$$

where i_{co0} is the average inductor current for the period T_P at the current value τ, Δi is the deviation of the current value from the average value. The maximum value of k_{Pimax} occurs at τ=0.5, which in this case corresponds to the current angle θ_1:

$$\theta_1=\arcsin(\frac{\tau}{K_M})=\arcsin(\frac{0,5}{0,93})=0,568\,(31,6\ grad) \qquad (22)$$

in this case, the current value $I_{co}(\theta_1)=I_{coм}\sin\theta_1$ will be 15.6 A. The effective current of the choke I_L when pulsations are neglected has the value $I_L=I_{com}/\sqrt{2}$=29,1·0,707=20,6 A.

As the choke core, we will choose a sendust toroidal core of the type MS-250060-2 from Micrometals, Inc. [23] with the parameters: outer diameter a =63.5 mm, inner diameter b =31.4 mm, thickness c =25.0 mm, magnetic line length l_μ=14.4 cm, cross-sectional area F_c =3.89 cm2, volume V_c =55.8 cm3, mass m_c =320 g, magnetic permeability μ = 60, approximate cost $(3-4).

Assuming current density $j=3\cdot10^6$ A/m2, for an effective current I_L =20.6 A, we obtain a cross-sectional area of a round wire F_w = 6.9 mm^2 and a diameter d_w = 2.96 mm, the nearest standard d_w = 2.83 mm. On the inner diameter, $w=(\pi b)/d_w=(\pi\cdot31,4\cdot10^{-3})/2,83\cdot10^{-3}\approx35$ turns can be placed in one layer. According to the specification, the specific inductance is 206 nH/w², then $L=252\cdot10^{-6}$ H. The amplitude of induction at a frequency of 50 Hz $B_{m(50)}$ at a current $I_{вт}$ =29.1 A will be:

$$B_{m(50)}=\frac{L\cdot I_{вт}}{F_c\cdot w}=\frac{2,52\cdot10^{-4}\cdot29,1}{6,3\cdot10^{-4}\cdot35}=0.539\,T\ , \qquad (23)$$

which is approximately half the saturation induction $B_S\approx1$ T [24].

From (21) at τ=0,5, we can find the value $\Delta i_м$ of the maximum deviation from the current value of the fundamental harmonic of the current $I_{co}(\theta_1)$=15,6 A:

$$\Delta i_м=\frac{U_d}{2\cdot L\cdot4\cdot f_П}=\frac{333}{2\cdot2,52\cdot10^{-4}\cdot4\cdot50000}=3,3A \qquad (24)$$

Let us estimate the power of losses in the core. It was indicated above that in the spectrum of the inductor current there are two higher harmonics of the current with frequencies (50±0,05) kHz, which create a "beat" of the current. It is known that losses in the core with a sinusoidal form of induction depend on the amplitude of the induction (in the case of a sendust – quadratically [24]), while the core induction is proportional to the current. With a non-sinusoidal form of the current, the resulting losses can be found as the sum of losses from individual harmonics [25]. Let us assume that in the vicinity of τ = 0,5 the total current of these harmonics gives a triangular pulse with an amplitude according to (24), and the contribution of both harmonics is the same: the current increase provided by each is half the value. Let us replace the real current curve of the triangular form with sinusoidal signals according to the criterion of equality of the effective values of the sinusoidal and triangular signals. For a triangle with amplitude $I_{мтр}$, the effective value of $I_{тр}$ is $I_{тр}=I_{мтр}/\sqrt{3}$, for a sinusoidal pulse of the same duration with amplitude $I_{мsin}$, the effective

ISSN 2079-5459 (print)
ISSN 2413-4295 (online)

value is $I_{мsin}/\sqrt{2}$. Equating the effective values, we obtain the value of the correction factor: $I_{мsin}=I_{mp}\cdot(2/3)^{0,5}=I_{mp}\cdot 0,82$. Then the amplitude of the equivalent sinusoid of one higher harmonic of the current:

$$I_{мsin1}=(\Delta i_{м}\cdot 0,82)/2=(3,3\cdot 0,82)/2=1,35\ A. \quad (25)$$

The amplitude of this component of the $B_{мsin1}$ induction in the core:

$$B_{мsin1}=\frac{\mu_0\cdot\mu\cdot I_{мsin1}\cdot w}{l_{\mu}}=\frac{1,256\cdot 10^{-6}\cdot 60\cdot 1,35\cdot 35}{14,4\cdot 10^{-2}}=0,025\ T.$$

Let us replace two harmonics with one equivalent harmonic of induction with frequency f_M =50000 Hz and amplitude $B_{мsin(eq)}$, which is equal to the square sum of these harmonics:

$$B_{мsin(eq)}=\sqrt{2\cdot B_{мsin1}^2}=B_{мsin1}\cdot\sqrt{2}=0,025\cdot\sqrt{2}=0,035\ T$$

According to the specification for the core material, the specific losses $P_P(B_{мsin1(eq)})$ for a frequency of 50 kHz for such an induction amplitude are 40 kW/m^3. With a core mass m_c =0.32 kg and a volume V_c=55.8 cm³=55,8·10^{-6} m^3, the losses in the core P_c will be:

$$P_c=P_P(B_{мsin(eq)})\cdot V_c=40\cdot 10^3\cdot 55,8\cdot 10^{-6}=2,23\ W \quad (26)$$

We also take into account the losses in the core from the induction component of the frequency 50 Hz (amplitude $B_{m(50)}$=0.54 T). According to the specification [24], the specific losses depend on the induction amplitude quadratically, and on the frequency as a power function with an index of 1.46, which gives the ratio of losses for frequencies 50 Hz and 50 kHz at the level of 5,4·10^{-3}, this allows us to neglect the former.

Estimation of ohmic losses. The length of one turn l_{w1}, the wire l_w, the winding resistance R_w and ohmic losses P_w:

$$l_{w1}=(a-b+2\cdot c)=63.5\cdot 10^{-3}-31.4\cdot 10^{-3}+2\cdot 25.4\cdot 10^{-3}=0.082\ м$$

$$l_w=l_{w1}\cdot w=0,082\cdot 35=2.87\ \ м$$

$$R_w=\frac{l_w\cdot\rho}{F_w}=\frac{2.87\cdot 2,1\cdot 10^{-8}}{6,29\cdot 10^{-6}}=9,59\cdot 10^{-3}\ \Omega$$

$$P_w=I_L^{\ 2}\cdot R_w=20,6^2\cdot 9,59\cdot 10^{-3}=4.06\ W$$

The estimation of additional losses in the winding (eddy current losses) was carried out according to the method [26]. It was found that to ensure the value of additional losses at the level of 10%, a winding of 5 insulated copper wires with a diameter of 1.2 mm should be made. Taking into account the 10% increase in losses in the winding, the total losses in it P_{wtot} will be P_{wtot} =4.47 W. Total losses in the P_L choke:

$$P_L=P_c+P_{wtot}=2,23+4,47=6,7\ W \quad (27)$$

To estimate the required capacitance of the filter capacitor C_1, we replace the currents of its harmonics with frequencies $f_M\pm f_G$ (i.e., the harmonics of the choke current) with the equivalent effective current of one harmonic I_{C1} with frequency f_M:

$$I_{C1}=\sqrt{2\cdot(I_{мsin1}/\sqrt{2})^2}=I_{мsin1}=5,52\ A \quad (28)$$

Let us take the amplitude of the equivalent sinusoid of the capacitor voltage $U_{C1м}$ at a frequency of f_M =50 kHz at the level of 2% of the amplitude of the fundamental harmonic (frequency f_G =50 Hz), i.e. from $U_{Gм}$ = 311 V, and then the effective value of U_{C1}:

$$U_{C1м}=0,02\cdot U_{Gм}=0,02\cdot 311=6,22\ V$$

$$U_{C1}=\frac{U_{C1м}}{\sqrt{2}}=\frac{6,22}{\sqrt{2}}=4,4\ V \quad (29)$$

Capacitor capacity *C1*:

$$C1=\frac{I_{C1}}{2\cdot\pi\cdot f_M\cdot U_{C1}}=\frac{5,52}{2\cdot\pi\cdot 50\cdot 10^3\cdot 4,4}=3,99\cdot 10^{-6}\ F \quad (30)$$

A film capacitor with a capacity of 10 μF is suitable.

Discussion of results and conclusion

Assuming that the ohmic losses in the inductor winding of the DC-DC converter are approximately the same as the losses in the inductor of an voltage-source inverter, i.e. about 7 W, we can estimate the losses in the DC-DC converter as the sum of the losses in the diode, transistor and inductor: $P_{ППП}=P_{VT}+P_{VD}+P_L$=8,53+3,4+7=19,3 W, which is 19.3/4512=0.43% (in NOCT mode), i.e. the efficiency is about 99.7%. For an voltage-source inverter, the total losses in the transistors and inductor are $P_{АІН}$=4 $P_{\Sigma}^{1}+P_L$ =49,6+6,7 = 56,3 W, i.e. 1.24%, and the efficiency is 98.8%. The total losses in the DC-DC converter and the voltage-source inverter for the load power supply mode with PV energy source in the NOCT $P_{DC/DC+DC/AC}$ mode will be 19.3+56.3=75.6 W, and the efficiency in this mode is 98.3%. In the autonomous battery power supply mode (in the absence of PV current) system efficiency is 98.8%. Comparing these parameters with the corresponding prototype indicators – 97.6%, and 94%, respectively, we can state a noticeable, from 97.6% to 98.3%., increase in efficiency for the load power supply mode from the PV, and a significant – from 94% to 98.8% increased efficiency for the load power supply mode in the absence of PV current. Power losses have been reduced by 1.4-5 times. The comparison is made with the basic structure [5] with a separate charge-discharge device relative to a low-voltage battery with a matching transformer. A noticeable increase in efficiency (from 97.6% to 98.3%) and reducing power losses by 1.4

times for the load power supply mode from PV is associated with the use of a modern element base of power devices – SiC MOSFET in the switch of the voltage-source inverter and DC-DC converter and Schottky diode in the DC-DC converter. Analyzing the ratio between static and dynamic losses of transistors (7.8 W to 0.55 W for a DC voltage converter and 11.2 W to 0.45 W for transistors of an voltage-source inverter), we can come to a conclusion about the feasibility of increasing (optimizing) the PWM frequency, which will allow us to optimize (improve) the weight, size and cost indicators of reactive components, including justifying the feasibility of using other magnetic materials for the choke of an voltage-source inverter (for example, sendust with a permeability of 125 instead of 60, which has approximately the same specific loss indicators). Optimization of the parameters of reactive elements when optimizing the conversion frequency will be one of the directions of further work, as well as consideration of the operation of voltage-source inverter and evaluation of the corresponding parameters of the converter in the regenerative rectifier mode when charging the battery from an alternating voltage network.

Gratitude

This work was carried out as part of a grant project EURIZON FELLOWSHIP PROGRAMME: “Remote Research Grants for Ukrainian Researchers” 2023. Grant Agreement #EU-3032.

Список літератури

1. Renewables 2023. *International Energy Agency*. 2024. URL: https://www.iea.org/reports/renewables-2023 (дата звернення: 01.06.2024).
2. Vignesh R., Feldman D., Desai J., Margolis R. *U. S. Solar Photovoltaic System and Energy Storage Cost Benchmarks: Q1 2021*. Golden, CO: National Renewable Energy Laboratory 2021. URL: https://www.nrel.gov/docs/fy22osti/80694.pdf (дата звернення: 01.06.2024).
3. Meban B., Donoghue T. O., Murdoch L. Global Market Outlook for Solar Power 2023-2027. *Solar Power Europe*. 2023. URL: https://www.solarpowereurope.org/insights/outlooks/global-market-outlook-for-solar-power-2023-2027/detail (дата звернення: 01.06.2024).
4. Gorjian S., Shukla A. *Photovoltaic solar energy conversion. Technologies, Applications and Environmental Impacts*. Elsevier Inc. 2020. doi 10.1016/C2018-0-05265-2
5. *Kstar BluE-H5/H3 energy storage system. Installation, operation & maintenance manual.* Shenzhen Kstar New Energy Company Limited. 2021. URL: https://solectric-energy.pl/wp-content/uploads/2022/08/KSTAR-BluE-S-H3-and-H5-series-Residential-ESS-Installation-Operation-Maintenance-Manual-v2.0.pdf
6. Femia N., Petrone G., Spagnuolo G., Vitelli M. *Power Electronics and Control Techniques for Maximum Energy Harvesting in Photovoltaic Systems.* CRC Press, 2013. 366p.
7. Muhammad H. Rashid. *Power Electronics Handbook. 5th Edition.* Elsevier Inc, 2024. 1466 p. doi: 10.1016/C2021-0-02072-1
8. *Ultimate Guide to LiFePO4 Voltage Chart*. URL: https://appbattery.com/faq/ultimate-guide-to-lifepo4-voltage-chart/
9. Компанія Viatec. URL: https://viatec.ua
10. Zamaruiev V., Ivakhno V., Makarov V., Styslo B. Power Factor and Harmonic Distortion Determination for DC Power Lines. *2020 IEEE 4th International Conference on Intelligent Energy and Power Systems (IEPS)*. Istanbul, Turkey. 2020. P. 122–125. doi: 10.1109/IEPS51250.2020.9263172.
11. *Nominal Operating Cell Temperature.* URL: https://www.pveducation.org/pvcdrom/modules-and-arrays/nominal-operating-cell-temperature (дата звернення: 09.02.2025)
12. *PNGNH60-B8 470-500W 182.* URL: https://www.pnsolarpv.com/storage/uploads/mp4/202309/05/1693897277_6v6kjrd0ZQ.pdf (дата звернення: 10.02.2025).
13. IDH12G65C6. URL: https://www.infineon.com/dgdl/Infineon-IDH12G65C6-DS-v02_00-EN.pdf?fileId=5546d4625cc9456a015cd4b8049d2de5 (дата звернення: 10.02.2025).
14. *Infineon Technologies IDH12G65C6XKSA1*. URL: https://www.digikey.com/en/products/detail/infineon-technologies/IDH12G65C6XKSA1/7428094?s=N4IgTCBcDaIJIBEASBGMBxAbAVgMKZAF0BfIA (дата звернення: 10.02.2025).
15. *IMZA65R040M2H.* URL: https://www.infineon.com/dgdl/Infineon-IMZA65R040M2H-DataSheet-v01_00-EN.pdf?fileId=8ac78c8c8d2fe47b018dd63b64ee52dc (дата звернення: 10.02.2025).
16. *Infineon Technologies IMZA65R040M2HXKSA1*. URL: https://www.digikey.com/en/products/detail/infineon-technologies/IMZA65R040M2HXKSA1/22157702?s=N4IgTCBcDaIJIFkBaBBAbAVgEoAYAsOCYAEgAQgC6AvkA (дата звернення: 10.02.2025).
17. Holmes D. G., Lipo T. A. *Pulse Width Modulation For Power Converters. Principles and Practice.* Institute of Electrical and Electronics Engineers. 2003. 724 p.
18. Wu B. *High-Power Converters and AC Drives*. Wiley-IEEE Press. 2006. 352 p. https://picture.iczhiku.com/resource/eetop/wyIhEulJPloRQmCc.pdf
19. Ивахно В. В., Замаруев В. В., Ильина О. В. *Выбор и расчет силовых полупроводниковых приборов полупроводникового преобразователя электрической энергии : учеб.метод. пособие*. Х.: НТУ «ХПИ», 2014. 70с.
20. Wintrich A., Nicolai U., Tursky W., Reimann T. *Application Manual Power Semiconductors*. Semikron: Innovation+ Service: Application Manual Power Semiconductors. ISLE Verlag. 2015. 452 p.
21. Макаров В. А., Замаруев В. В., Ивахно В. В., Ластовка А. П. К вопросу выбора частоты синусоидальной ШИМ источника резервного питания при его работе на линейную и нелинейную нагрузку. *Технічна електродинаміка.* 2009. Ч. 5. С. 43–46.
22. Гончаров Ю. П., Панасенко М. В., Семененко О. І., Хворост М. В. *Статичні перетворювачі тягового рухомого складу: навч. посібник*. Харків: НТУ "ХПІ", 2007. 192 с.

ISSN 2079-5459 (print)
ISSN 2413-4295 (online)

23. *Micrometals*. URL: https://datasheets.micrometals.com/MS-250060-2-DataSheet.pdf (дата звернення: 09.02.2025)
24. *Сердечники из материала Sendust, Kool Mμ, Альсифер*. URL: https://coretech.com.ua/docs/coretech_sendust_cores_[2012].pdf (дата звернення: 09.02.2025)
25. Тьомкіна Л. М. *Методичні вказівки до практичних занять та самостійної роботи з дисципліни «Елементи магнітної техніки» для студентів спеціальності 20.05 «Промислова електроніка»*. Харків: ХПІ, 1990. 62 с.
26. Гончаров Ю. П., Будьонний О. В., Морозов В. Г., Панасенко М. В., Ромашко В. Я., Руденко В. С. *Перетворювальна техніка*. Ч.2. Підручник. Харків: «ФОЛІО», 2000. 300 с.

References (transliterated)

1. Renewables 2023. *International Energy Agency*, 2024. Available at: https://www.iea.org/reports/renewables-2023 (accessed 01.06.2024).
2. Vignesh R., Feldman D., Desai J., Margolis R. *U.S. Solar Photovoltaic System and Energy Storage Cost Benchmarks: Q1 2021*. Golden, CO. National Renewable Energy Laboratory, 2021. Available at: https://www.nrel.gov/docs/fy22osti/80694.pdf (accessed 01.06.2024).
3. Meban B., Donoghue T. O., Murdoch L. Global Market Outlook for Solar Power 2023-2027. *Solar Power Europe*, 2023. Available at: https://www.solarpowereurope.org/insights/outlooks/global-market-outlook-for-solar-power-2023-2027/detail (accessed 01.06.2024).
4. Gorjian S., Shukla A. (Eds.). *Photovoltaic Solar Energy Conversion. Technologies, Applications and Environmental Impacts*. Elsevier Inc., 2020, doi: 10.1016/C2018-0-05265-2.
5. *Kstar BluE-H5/H3 energy storage system. Installation, operation & maintenance manual*. Shenzhen Kstar New Energy Company Limited. 2021. Available at: https://solectric-energy.pl/wp-content/uploads/2022/08/KSTAR-BluE-S-H3-and-H5-series-Residential-ESS-Installation-Operation-Maintenance-Manual-v2.0.pdf(accessed 09.02.2025).
6. Femia N., Petrone G., Spagnuolo G., Vitelli M. *Power Electronics and Control Techniques for Maximum Energy Harvesting in Photovoltaic Systems*. CRC Press, 2013, 366p.
7. Muhammad H. Rashid. *Power Electronics Handbook*. 5th Edition. Elsevier Inc., 2024. 1466 p., doi: 10.1016/C2021-0-02072-1.
8. *Ultimate Guide to LiFePO4 Voltage Chart*. Available at: https://appbattery.com/faq/ultimate-guide-to-lifepo4-voltage-chart/ (accessed 09.02.2025).
9. Viatec. Available at: https://viatec.ua.
10. Zamaruiev V., Ivakhno V., Makarov V., Styslo B. *Power Factor and Harmonic Distortion Determination for DC Power Lines*. *2020 IEEE 4th International Conference on Intelligent Energy and Power Systems (IEPS)*, Istanbul, Turkey, 2020, pp. 122–125, doi: 10.1109/IEPS51250.2020.9263172.
11. *Nominal Operating Cell Temperature*. Available at: https://www.pveducation.org/pvcdrom/modules-and-arrays/nominal-operating-cell-temperature (accessed 09.02.2025).
12. *PNGNH60-B8 470-500W 182*. Available at: https://www.pnsolarpv.com/storage/uploads/mp4/202309/05/1693897277_6v6kjrd0ZQ.pdf (accessed 10.02.2025).
13. *IDH12G65C6*. Available at: https://www.infineon.com/dgdl/Infineon-IDH12G65C6-DS-v02_00-EN.pdf?fileId=5546d4625cc9456a015cd4b8049d2de5 (accessed 10.02.2025).
14. *Infineon Technologies. IDH12G65C6XKSA1*. Available at: https://www.digikey.com/en/products/detail/infineon-technologies/IDH12G65C6XKSA1/7428094?s=N4IgTCBcDaIJIBEASBGMBxAbAVgMKZAF0BfIA (accessed 10.02.2025).
15. *IMZA65R040M2H*. Available at: https://www.infineon.com/dgdl/Infineon-IMZA65R040M2H-DataSheet-v01_00-EN.pdf?fileId=8ac78c8c8d2fe47b018dd63b64ee52dc (accessed 10.02.2025).
16. *Infineon Technologies. IMZA65R040M2HXKSA1*. Available at: https://www.digikey.com/en/products/detail/infineon-technologies/IMZA65R040M2HXKSA1/22157702?s=N4IgTCBcDaIJIFkBaBBAbAVgEoAYAsOCYAEgAQgC6AvkA (accessed 10.02.2025).
17. Holmes D. G., Lipo T. A. *Pulse Width Modulation for Power Converters. Principles and Practice*. Institute of Electrical and Electronics Engineers, 2003. 724 p.
18. Wu B. *High-Power Converters and AC Drives*. Wiley-IEEE Press, 2006. 352 p. Available at: https://picture.iczhiku.com/resource/eetop/wyIhEulJPloRQmCc.pdf.
19. Ivakhno V. V., Zamaruiev V. V., Ilina O. V. *Vybor i raschet silovykh poluprovodnikovykh priborov poluprovodnikovogo preobrazovatelya elektricheskoy energii: ucheb.-metod. posobie* [Selection and Calculation of Power Semiconductor Devices of a semiconductor electric energy converter: educational and methodical manual]. Kharkiv: NTU "KhPI", 2014. 70 p.
20. Wintrich A., Nicolai U., Tursky W., Reimann T. *Application Manual Power Semiconductors*. Semikron: Innovation+ Service, ISLE Verlag, 2015. 452 p.
21. Makarov V. A., Zamaruiev V. V., Ivakhno V. V., Lastovka A. P. K voprosu vybora chastoty sinusoidal'noy ShIM istochnika rezervnogo pitaniya pri ego rabote na lineynuyu i nelineynuyu nagruzku [On the Issue of Selecting the Frequency of Sinusoidal PWM of a Backup Power Source When Operating on Linear and Nonlinear Load]. *Tekhnichna elektrodynamika [Technical Electrodynamics]*, 2009, no. 5, pp. 43–46.
22. Goncharov Yu. P., Panasenko M. V., Semenenko O. I., Khvorost M. V. *Statychni peretvoriuvachi tiahovogo rukhomogo skladu: navch. posibnyk [Static Converters of Traction Rolling Stock: Textbook]*. Kharkiv. NTU "KhPI", 2007. 192 p.
23. *Micrometals*. Available at: https://datasheets.micrometals.com/MS-250060-2-DataSheet.pdf. (accessed 09.02.2025).
24. *Serdechniki iz materiala Sendust, Kool Mμ, Alsifer* [Cores Made of Sendust, Kool Mμ, Alsifer Material]. Available at: https://coretech.com.ua/docs/coretech_sendust_cores_[2012].pdf. (accessed 09.02.2025).
25. Tjomkina L. M. *Metodychni vkazivky do praktychnykh zaniat ta samostiinoi roboty z dystsypliny «Elementy mahnitnoi tekhniky» dlia studentiv spetsialnosti 20.05 «Promyslova elektronika» [Methodical Instructions for Practical Classes and Independent Work in the Discipline "Elements of Magnetic Technology" for Students of Specialty 20.05 "Industrial Electronics"]*. Kharkiv. KhPI, 1990. 62 p.

26. Goncharov Yu. P., Budionnyi O. V., Morozov V. G., Panasenko M. V., Romashko V. Ya., Rudenko V. S. *Peretvoriuvalna tekhnika. Ch.2. Pidruchnyk [Conversion Technology. Part 2. Textbook]*. Kharkiv. "FOLIO", 2000. 300 p.

Відомості про авторів (About authors)

Ivakhno Volodymyr – Doctor of Technical Sciences, Docent, Professor, Department of Power and biomedical electronics, National Technical University "Kharkiv Polytechnic Institute", Kharkiv, Ukraine, ORCID: 0000-0002-2122-6151; e-mail: Volodymyr.Ivakhno@khpi.edu.ua

Івахно Володимир Вікторович – доктор технічних наук, доцент, Національний технічний університет «Харківський політехнічний інститут», професор кафедри «Промислова і біомедична електроніка»; м. Харків, Україна; ORCID: 0000-0002-2122-6151; e-mail: Volodymyr.Ivakhno@khpi.edu.ua**.**

Zamaruiev Volodymyr – Candidate of Technical Sciences, Docent, Professor, Department of Power and biomedical electronics, National Technical University "Kharkiv Polytechnic Institute", Kharkiv, Ukraine, ORCID: 0000-0003-0598-5673; e-mail: Volodymyr.Zamaruiev@khpi.edu.ua

Замаруєв Володимир Васильович – кандидат технічних наук, доцент, Національний технічний університет «Харківський політехнічний інститут», професор кафедри «Промислова і біомедична електроніка»; м. Харків, Україна; ORCID: 0000-0003-0598-5673; e-mail: Volodymyr.Zamaruiev@khpi.edu.ua

Plakhtii Oleksandr – Candidate of Technical Sciences, Docent, Associate Professor, Department of electrical power engineering, electrical engineering and electromechanics, Ukrainian state university of railway transport, Kharkiv, Ukraine; ORCID: 0000-0002-1535-8991; e-mail: a.plakhtiy1989@gmail.com

Плахтій Олександр Андрійович – кандидат наук, доцент, кафедра електроенергетики, електротехніки та електромеханіки, Український державний університет залізничного транспорту, Харків, Україна; ORCID: 0000-0002-1535-8991; e-mail: a.plakhtiy1989@gmail.com

Vinnikov Dmitri – Ph. D., Professor DrS, Department of Electrical Power Engineering and Mechatronics, Tallinn University of Technology, Tallinn, Estonia; ORCID: 0000-0001-6010-3464; e-mail: dmitri.vinnikov@taltech.ee.

Винников Дмитро – Ph.D., професор кафедри «Електроенергетика та мехатроніка» Талліннський технологічний університет, ТАЛТЕХ, Таллінн. Естонія. ORCID: 0000-0001-6010-3464; e-mail: dmitri.vinnikov@taltech.ee

Doluda Mykola – VIATEC company, head of the sales development group for energy-saving systems, Kyiv, Ukraine; e-mail m.doluda@viatec.ua.

Долуда Микола Володимирович – компанія VIATEC, керівник групи з розвитку продажів енергозберігаючих систем, м. Київ, Україна; e-mail m.doluda@viatec.ua.

Filipieva Maryna – Ph. D. student, Department of electrical power engineering, electrical engineering and electromechanics, Ukrainian state university of railway transport, Kharkiv, Ukraine; ORCID: 0000-0001-6499-7493; e-mail: marifil2603@gmail.com.

Філіп'єва Марина Віталіївна – аспірантка, кафедра електроенергетики, електротехніки та електромеханіки, Український державний університет залізничного транспорту, Харків, Україна; ORCID: 0000-0002-1535-8991; e-mail: marifil2603@gmail.com

Будь ласка, посилайтесь на цю статтю наступним чином:

Івахно В. В., Замаруєв В. В., Плахтій О. А., Винников Д., Долуда М. В., Філіп'єва М. В. Підвищення ефективності побутової автономної сонячної електростанції потужністю 5 кВт без окремого зарядного конвертора. *Вісник Національного технічного університету «ХПІ». Серія: Нові рішення в сучасних технологіях*. – Харків: НТУ «ХПІ». 2025. № 1 (23). С. 19-31. doi:10.20998/2413-4295.2025.01.03.

Please cite this article as:

Ivakhno V., Zamaruiev V., Plakhtii O., Vinnikov D., Doluda M., Filipieva M. Increasing the efficiency of a 5 kW home autonomous solar power plant without a separate charging converter. *Bulletin of the National Technical University "KhPI". Series: New solutions in modern technology*. – Kharkiv: NTU "KhPI", 2025, no. 1(23), pp. 19–31, doi:10.20998/2413-4295.2025.01.03.

Надійшла (received) 20.02.2025
Прийнята (accepted) 21.03.2025